employed. More generally these results imply that it may be possible to substitute the wave functions of the unexcited ion of the next higher atomic number for the wave functions of the ion of interest excited in an x-ray state when the latter are unknown. However, if such substituted wave functions are to be employed, it would be preferable to use the wave functions of the unexcited ion instead of those of the next atom for all electrons in the same shell as the excited electron and for all inner shells.

The authors wish to thank Miss Cynthia W. Wyeth for her help at several points with the calculations.

PHYSICAL REVIEW VOLUME 98, NUMBER 4 MAY 15, 1955

Experimental Cross Section for Photodetachment of Electrons from H^- and D^-†

LEWIS M. BRANSCOMB AND STEPHEN J. SMITH
National Bureau of Standards, Washington, D. C.

(Received January 3, 1955)

The photodetachment of electrons from atomic hydrogen negative ions has been studied, and the integrated cross section measured by using the radiation from a tungsten filament at 3300°K in a modulated crossed-beam experiment. The wavelength dependence of the cross section is measured from 4000 to about 9000 A by using sharp-cut glass filters. The ratio of the experimental integrated cross section to the value predicted theoretically by Chandrasekhar is 1.01, with a 2 percent reproducibility and 10 percent upper limit to the systematic errors.

I. INTRODUCTION

THE departures of the continuous solar spectrum, in the region between 0.6 and 1.6 microns, from the Planck curve characteristic of a black body were first ascribed by Wildt[1] to the continuous absorption of the H^- ions in the solar photosphere. The electron affinity of H^- is about 0.75 ev and the ion has only one bound state. Hence the absorption of visible and near-infrared radiation leads to photodetachment, described by the equation

$$H^- + h\nu \rightarrow H + e^-. \tag{1}$$

The calculation of the cross section, σ, for this process has been undertaken with great diligence,[2] the most detailed and modern calculations being those of Chandrasekhar.[3] This calculated cross section rises from a threshold at 1.65 microns to a maximum of 4.52×10^{-17} cm^2 at 8275 A. The theoretical values give a basis for consistent agreement between the predicted absorption coefficient of the solar photosphere and the observed solar spectrum.[4]

Until recently[5] negative-ion photodetachment had not been detected in laboratory studies, although Lochte-Holtgreven[6] has reported that the reverse process, radiative attachment, contributes to the continuous emission from a high-current arc discharge. Although one can calculate the cross section for photodetachment from that for radiative attachment by using the principle of detailed balancing,[2] the circumstances of Lochte-Holtgreven's arc measurement do not permit direct evaluation of the cross section. Fite[7] attempted in 1950 to detect photodetachment from H^-. His experiment, although not successful in demonstrating photodetachment, led to the development of the high-current negative ion source[8] used in this experiment, and helped determine the present experimental approach. Photodetachment was observed in this laboratory in 1953.[5] The present paper describes the quantitative results of a crossed-beam experiment yielding the integrated cross section and information about its wavelength dependence in the visible for photodetachment from H^- and D^-.

II. THEORY OF THE EXPERIMENTAL METHOD

When one crosses a beam of H^- ions with a beam of very intense radiant energy of suitable wavelength, photons are absorbed, ions destroyed, and electrons liberated. Since the available concentration of negative ions is very low and since the spectrum is continuous, the study of photodetachment is out of the reach of conventional absorption spectroscopy. When one modulates the light beam, photodetachment may be recognized as a small ripple in the dc ion beam. However,

† For various periods since its inception this research has been sustained by the Harvard University Society of Fellows and the Office of Naval Research, as well as by the National Bureau of Standards.

[1] R. Wildt, Astrophys. J. **89**, 295 (1939).
[2] H. S. W. Massey, *Negative Ions* (Cambridge University Press, London, 1950), second edition.
[3] S. Chandrasekhar, Astrophys. J. **102**, 395, 223 (1945); **100**, 176 (1944).
[4] D. Chalonge and V. Kourganoff, Ann. astrophys. **9**, 69 (1946); **13**, 347 (1950). J. A. Hynek, *Astrophysics; A Topical Symposium* (McGraw-Hill Book Company, Inc., New York, 1951).
[5] L. M. Branscomb and W. L. Fite, Phys. Rev. **93**, 651 (A) (1954).
[6] W. Lochte-Holtgreven, Naturwiss. **38**, 258 (1951).
[7] W. L. Fite, Ph.D. Dissertation, Harvard University, 1951 (unpublished).
[8] W. L. Fite, Phys. Rev. **89**, 411 (1953).

since the noise in a typical high-current ion beam is 1000 times shot noise at low frequencies,[8] we collect the very small alternating current of photodetached electrons produced in the region of intersection of the light and ion beams. In this case the photodetached electron current must be distinguished from the noise within the bandwidth of the amplifier arising from ions scattered in the residual gas, collisional detachment,[9] and noise from the amplifier itself.

The experiment is complicated by the fact that monochromatic light of sufficient intensity was not available, thus necessitating the measurement of integrated cross sections over a wide spectral range.

Consider an H^- ion moving in the x direction with a velocity v. At the point x it is illuminated with a normally incident radiant flux $\phi(x,\lambda)d\lambda$ ergs/cm^2-sec of parallel light in the wavelength range λ to $\lambda+d\lambda$. The probability that the ion will lose an electron in the distance dx is

$$P_x dx = (dx/vhc)\int \sigma(\lambda)\phi(x,\lambda)\lambda d\lambda. \qquad (2)$$

Let us define $\phi'(\lambda)$ as the normalized radiant flux so that

$$\phi(x,\lambda)=\phi'(\lambda)w(x)/s. \qquad (3)$$

Here s is a small distance perpendicular to the ion beam, larger than the ion beam, but small enough so that the light intensity is reasonably constant over this distance, and $w(x)/s$ is the power density at the ion beam. Then the probability of detachment when the ion passes a distance L through the light beam is

$$P=(hcvs)^{-1}\int_\lambda \sigma(\lambda)\phi'(\lambda)\lambda \int_x w(x)dxd\lambda$$

$$=W(hcvs)^{-1}\int_\lambda \sigma(\lambda)\phi'(\lambda)\lambda d\lambda. \qquad (4)$$

TABLE I. $P_{\text{theor}}E^{\frac{1}{2}}/\overline{W}$ for nine filters with new[a] tungsten lamps. E is ion energy in ev; $\overline{W}$ is the radiant power in the ion beam; and P_{theor} is the detachment probability [Eq. (5)] calculated from Chandrasekhar's cross section.[b]

Corning filter No.	Approximate cutoff (A)	$P_{\text{theor}}E^{\frac{1}{2}}/\overline{W}\ 10^5$
3389	4200	7.000
3385	4800	7.381
3486	5300	7.287
3482	5500	7.113
2424	5900	7.239
2412	6100	6.798
2030	6600	6.625
2550	~8500	4.671
2540	~9900	3.368

[a] After five to ten hours operation the evaporated tungsten (Fig. 1) causes a ~1 percent decrease from the given values.
[b] See reference 3.

[9] J. B. Hasted, Proc. Roy. Soc. (London) **212**, 235 (1952).

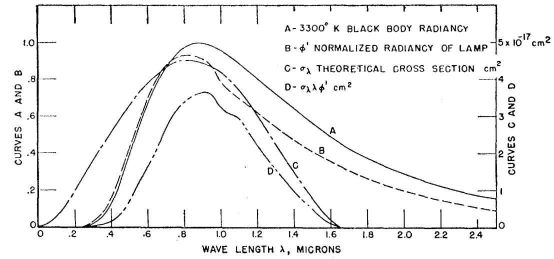

FIG. 1. Wavelength dependent quantities required for calculation of the photodetachment probability in H^- for radiation from the tungsten lamp with no filters. Curve A is normalized to unity at the maximum; curve B is normalized to unit radiant power. Curves B and D show a small dip due to evaporated tungsten and not present in new lamps.

Here $W=\int_0^L w(x)dx$ and is the total power incident on the area sL. This expression is independent of L providing only that $L \geqslant$ width of the light beam (i.e., $\phi=0$, $x>L$ and $x<0$). In practice s and L are the dimensions of the radiometer with which W is measured.

If a current i of ions and a current j of electrons are drawn from the illuminated region, $P_{\text{exp}}=j/i$. If we use sinusoidally chopped light of time average power $\overline{W}$ in the area sL,

$$P=\bar{j}/i=(\overline{W}/hcvs)\int \sigma(\lambda)\phi'(\lambda)\lambda d\lambda. \qquad (5)$$

A measurement of $\bar{j}$ and i gives the experimental probability of detachment per ion (P_{exp}). We can also calculate this probability (P_{theor}) from the theoretical cross section σ, the known spectral distribution of the light ϕ', the measured power $\overline{W}$, ion velocity v, and the vertical dimension s of the rectangular instrument (area sL) used to measure $\overline{W}$. Thus, the experiment consists of a comparison of P_{exp} with P_{theor}. Equation (5) has been written so that the integral can be evaluated numerically and is independent of the parameters which may be varied in the experiment ($\overline{W},s,v$), provided that a source of sufficient spectral stability is available. Figure 1 shows the form of the wavelength-dependent functions for H^-.

To gain additional information about the wavelength dependence of $\sigma(\lambda)$ we may insert sharp cutoff filters of normalized transmission $T(\lambda)$ in the light beam. For each filter, $\int \sigma\phi' T\lambda d\lambda$ is evaluated, so that the successive ratios $P_{\text{exp}}/P_{\text{theor}}$ for the filters reflect the accuracy of the theoretical cross section in the vicinity of the filter cutoff. Table I gives the values of this integral for nine filters.

III. EXPERIMENTAL METHOD

Figure 2 is a block diagram of the apparatus, a detailed description of which will be published elsewhere.

A. Ion Beam

The ion source is an adaptation of the dc glow discharge source described by Fite,[8] in which electrons and

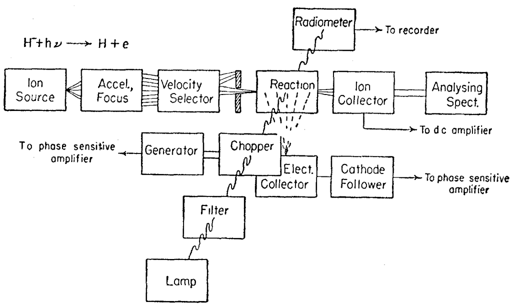

FIG. 2. Diagram of the crossed beam experiment. The generator produces a reference signal of adjustable phase for the phase detector. The electron current is extracted from the illuminated ion beam with weak inhomogeneous electric and magnetic fields in the reaction chamber.

negative ions are extracted from the striated positive column through a 0.015 in.×0.100 in. channel in a conical aluminum anode. A 3-mm aluminum aperture is allowed to float in the positive column immediately in front of the anode cone. The high electron mobility charges this aperture slightly negative with respect to the plasma and assists in increasing the axial concentration of negative ions. The cathode of the discharge is a 1 in.×2 in. Al or Ni cylinder. A dc voltage of 2 to 10 kv is applied across the discharge in series with a 240 000-ohm stabilizing resistance. Typical discharge current is 15 ma.

After emerging from the anode with about 100-ev energy, the negative ions are focussed by an electrostatic coaxial cylinder lens down the axis of the crossed field velocity selector. Helmholtz coils, external to the vacuum system, are available to supply slight corrections to the alignment of the ion beam. Those ions for which the velocity selector produces no transverse displacement pass through three 0.25-in. circular apertures and into the detachment chamber with an energy which may be chosen between 50 and 400 ev.

The apertures permit differential pumping to minimize gas scattering and collisional detachment. The main chamber, containing the velocity selector, is evacuated with a 200-l/sec mercury diffusion pump. The detachment chamber is evacuated with a 50-l/sec pump, whose fore pressure is provided by the main vacuum. The typical operating pressures are 10^{-5} mm in the main chamber and 10^{-6} mm in the detachment chamber.

The detachment chamber is shown schematically in Fig. 3. The ion beam is collected in the Faraday cup at the right. Secondary electron emission is suppressed by a weak transverse magnetic field and on some measurements by a 1.5-volt bias on the collector. A magnetic shutter in the back of the ion collector can permit the ion beam to pass into a 90° sector analyzer for high-resolution mass analysis of the beam. With this aperture closed the time-average ion current is measured with a dc amplifier. For measurements of ion energy an adjustable stopping potential is applied to this collector.

B. Light Beam

A 1-kilowatt projection lamp with a biplane coiled tungsten filament (GE 1 kw T-12 C13D) operating at a color temperature of 3420°K meets the stringent requirement of spectral stability and has a spectral distribution in convenient correspondence with the theoretical cross section (Fig. 1). The manner in which this distribution is determined is described in Part IV.

Radiation from the lamp is focussed by a 6-inch diameter front-aluminized spherical mirror through a 450-cps mechanical chopper and a quartz window, onto the negative ion beam. The image of the filament (which is approximately 1 cm^2 in area) is somewhat magnified and defocussed by the spherical mirror. Although wasteful of intensity, this defocussing helps meet the requirement that the intensity be homogeneous in the ~0.3-in. diameter of the beam. Of the 1-kw input power to the lamp, approximately 870 watts are radiated, of which about 30 watts are incident on the 0.400 in.×1.5 in. radiometer. A shield of highly polished aluminum foil with a 0.5 in.×1.5 in. aperture, not shown in Fig. 3, is installed inside the vacuum immediately in front of the ion beam. This prevents the radiation coming directly from the lamp filament at wide angles from scattering in the detachment chamber and falling on the back side of the radiometer.

The radiation is incident on the ion beam in a 35° cone and is not parallel, as assumed in the derivation of (5). If one takes proper account of this by replacing the ion velocity in (2) with $v\cos\theta$, where θ is the angle of incidence of a light ray on the ion beam, and writes in place of $\phi(x,\lambda)$ a reasonable angular-dependent function $\phi(x,\lambda,\theta)d\theta$, it can be shown that the error introduced by the assumption of parallelism is negligible. Sources of error due to light beam geometry were investigated by performing the experiment under a wide range of geometrical arrangements.

The radiometer is a copper "V" having a 45° apex angle. The inside surface is blacked with electrolytically deposited platinum. The back surface is covered with polished aluminum foil. Supporting this "V" and conducting the 30 watts of absorbed radiation to a water

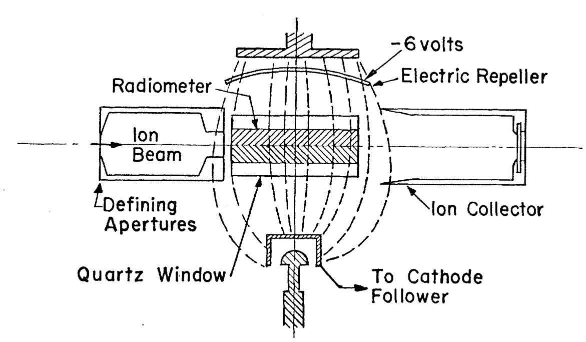

FIG. 3. Schematic of the detachment chamber. The dotted lines indicate the shape of the weak magnetic field used for trapping detached electrons. The electron collector is biased +15 volts.

cooled support, is a precisely machined 0.140-in. diameter bar of oxygen-free high-conductivity, copper. Two constantan wires imbedded in the bar 0.500 in. apart provide two thermocouple junctions, whose temperature difference multiplied by the known heat conductance of the OFHC copper bar provides an absolute measure of the heat energy conducted down the bar. The temperature rise in the radiometer results in radiation losses of about 9 percent. Although exact knowledge of the radiation loss and of the emissivity of the platinum-black would afford a direct measure of the total radiant power incident on the radiometer, the basic calibration is actually performed with standard lamps, as described in Part IV. These two methods of calibration give consistent results.

C. Detached Electron Current

In the region of intersection of the light and ion beams, weak inhomogeneous magnetic and electric fields extract the electrons by causing them to spiral down the magnetic flux lines as shown in Fig. 3. The magnetic field in the ion beam is about 50 gauss. A plate at the top of the detachment chamber is charged 7 volts negative to provide an electric field gradient in the beam. The electron collector, a cap above one pole of the magnet, is biased 15 volts positive. With this geometry, all free electrons generated in the illuminated portion of the ion beam are collected. (See Part V, Sec. D.) The collector is only 0.5-in. in diameter, thus presenting a small target to scattered ions. The predominant noise signal is due to electrons detached in gas collisions.

D. Electron Current Amplifier

With ion currents of 10^{-7} amp and 20 watts of radiation in the beam, modulated currents of photodetached electrons of the order of 10^{-12} amp are to be measured. The unmodulated collisionally-detached electron signal will be of the order of 10^{-11} amp at 10^{-6} mm pressure.[9] The modulated signal is measured by using a modified Baird Associates phase-sensitive detector with a minimum bandwidth of about 1/20 cps. The preamplifier is a 10^8-ohm input cathode follower using a VX-41A tetrode electrometer in triode connection. The chopping frequency of 450 cps is chosen as a compromise between the frequency limitation of the preamp input resistance (with a collector capacitance of about 3 $\mu\mu$f) and the reduction of ion beam noise with frequency.[8]

IV. CALIBRATIONS

A. Spectral Distribution

The projection lamps, after "breaking in," are tested[10] to determine the voltage at which the color temperature is 3420°K. The absolute temperature of the filament is then 3300°K. the reduction depending on the emissivity of tungsten in the visible.[11,12] The Planck curve for 3300°K is then multiplied by the measured transmission of the quartz lamp envelope and by the best available values of the emissivity of tungsten from 3000 A to 4 microns at 3300°K. These data are extrapolated in temperature from the definitive work of DeVos.[13] A partial check on the reliability of this procedure is had by calculating the power attenuation to be expected when each of the nine sharp cutoff filters is interposed in the light beam. This result is compared with the actual attenuation measured by the radiometer. The transmission of each filter is calibrated in the visible[10] and in the infrared.[14] The principal uncertainty in the filter transmissions is caused by the high temperature rise in the glass. The deep red filters usually shatter after a few minutes, in spite of air blast cooling. Systematic errors in $\phi'(\lambda)$ are thought to contribute no more than 2 percent to the error in our results.

B. Radiometer

Several of the projection lamps were calibrated for total radiant power[14] in microwatts/cm^2 at two meters in the direction perpendicular to the plane of the filament. Each lamp was then placed a known distance from the radiometer, with the mirror removed. The radiation incident on the radiometer was then calculated from the solid angle subtended. Corrections were made for the change in intensity with angle from the lamp, for the reflection from the quartz window, and for the attenuation of two very fine knitted tungsten mesh screens, which prevent the accumulation of static charges on the window. For distances of 2 in. to 12 in. from lamp to radiometer the inverse square law is obeyed, thus demonstrating the linearity of the radiometer and the absence of internal reflections in the detachment chamber. Further demonstration of radiometer linearity is obtained by calibrating a lamp for radiant power at 120 and 105 volts and checking the ratio of these powers with our radiometer.

The reliability of the standardization of the lamp is given as within 2 percent by the Radiometry Section. With 3 percent allowed for the calibration of the radiometer with this lamp, the value of $\bar{W}$ in (5) is thought to have systematic errors no greater than 5 percent.

C. Electron Current Amplifier

The electron current is measured with an amplifier whose gain depends on careful phase-matching and is sensitive to phase shifts. The distributed capacity of the preamplifier input makes it most convenient to calibrate the complete electron current amplifier system by using

[10] Measured by the NBS Photometry and Colorimetry Section.

[11] *Handbook of Chemistry and Physics* (Rubber Publishing Company, Cleveland, 1953), thirty-fifth edition, p. 2466.
[12] D. B. Judd, J. Research Natl. Bur. Standards **44**, 1 (1950).
[13] J. C. DeVos, Physica **20**, 690 (1954).
[14] Measured by the NBS Radiometry Section.

photoelectrons artificially produced in the detachment chamber. The chopped ultraviolet light from a low-pressure mercury discharge (ozone lamp) produces the photoelectrons. The output of the amplifier is compared with the average photocurrent, measured by floating the entire cathode follower on the 10^4-ohm input of a dc amplifier. This calibration procedure is carried out at about 10-minute intervals during the taking of data. Steady drifts in gain of about 1 percent in each interval are often encountered.

D. Wave Form

Because the amplifier has a very narrow bandwidth, the output detects only that part of the detached electron current or calibrating signal which is in the fundamental frequency. Therefore the wave form of the calibrating signal and of the radiation from the projection lamp must be recorded. This is done while driving the chopper at a very slow rate. Then the first Fourier coefficients of the two wave forms are determined by numerical integration to obtain the corrections for the average electron current, $\bar{j}$, and the light power, $\bar{W}$.

V. APPARATUS PERFORMANCE

A. Operation of the Source

Ion beams of up to 1 μa of H^-, OH^-, O^- and O_2^- have been collected, after mass separation in the velocity selector, with the source discharge operating in the neighborhood of 100 microns pressure and with two or three striations in the positive column. The yield of H^- ions in a dry hydrogen discharge is quite low,[8,15] but the role of the water vapor which must be added for good yields is not clear. In order to find the ratios of H_2 and H_2O concentrations for optimum H^- generation, beams from H_2 wet with D_2O were examined. The results, shown in Table II, are only qualitative, for the striations move with changes in concentration, requiring changes of total pressure and voltage to restore the ion beam. Table II shows that small amounts of D_2O increase the H^- yield, and that D^- ions result directly from water. The largest beams were obtained not in pure water vapor, but in wet hydrogen, as shown in Table II, and as found by Fite.[8] The most abundant ion from pure water discharges is OH^-. H^- and O_2^- yields are about three times smaller, and a trace of O^- is seen. At these relatively low pressures it seems likely that the OH^- is created directly by dissociative attachment,[16] although this seems to be inconsistent with the recent theoretical treatment by Laidler.[17]

TABLE II. Negative ion currents extracted at the anode of a low-pressure glow discharge using mixtures of D_2O and H_2.

Pressure (mm of Hg) at leak to discharge		Ion current (μa)				
D_2O	H_2	H^-	D^-	OD^-	O_2^-	D^-+H^-
20	0	0.001	0.031	0.13	0.01	0.032
20	30	0.008	0.029			0.037
20	85	0.0245	0.017	(not measured)		0.041
~10	85	0.020	0.0065			0.0265
~1	85	0.006	0.00040			0.0064
0	85	0.0051	0.00025	0.0012	0.0009	0.0052

[15] W. H. Bennett and P. F. Darby, Phys. Rev. 49, 97 (1936).

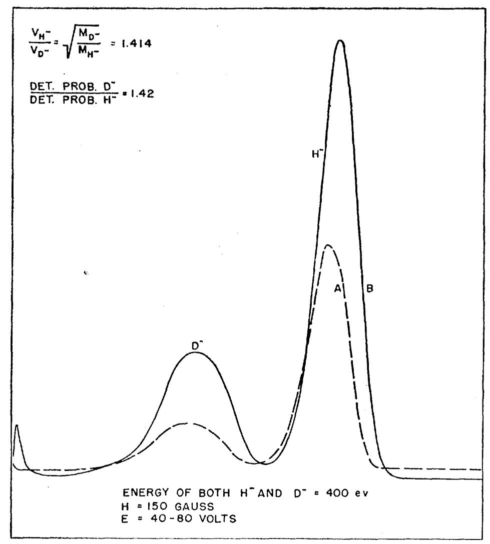

FIG. 4. Velocity selector scan obtained by varying the E-field from 40–80 volts while holding the magnetic field constant. The measured detachment probabilities for H^- and D^- are in the inverse ratio of the ion velocities, as expected since the two isotopes should have the same photodetachment cross sections.

The ions leave the anode of the wet H_2 discharge with about 90-ev energy and a 10–15 ev energy spread. The floating aperture lens described in Part II has very nearly the same potential as the region of the plasma from which the ions originate. Occasionally a second group of ions is observed with energies of about 150 ev, presumably from the second striation from the anode.

B. Velocity Selector

It is necessary to show that the velocity selector has sufficient resolving power to remove OH^- and other ions from the beam, and that the velocity is correctly measured and accounted for in Eq. (5). A mixed D^- and H^- beam of homogeneous energy was generated. With the projection lamp illuminating the beam and the detached electrons being recorded, the velocity selector was scanned across the D^- and H^- beams. Figure 4 shows the result. Within the accuracy of measurement the detachment probabilities are in the ratio of velocities, i.e., 1:1.414. The photodetachment cross sections for the two isotopes are, of course, identical within experimental accuracy.

Because the slower D^- ions give a larger photodetach-

[16] See reference 2, p. 76.
[17] K. J. Laidler, J. Chem. Phys. 22, 1740 (1954).

ment yield and are less subject to large angle scattering than H^-, they were used for most of the final results quoted in this paper.

C. Phase Adjustment and Photoelectric Effect

The only spurious effect not excluded by modulation is the photoelectric effect. Since the photoelectric effect is independent of ion current, photodetachment is measured by turning on and off the ion beam at constant light intensity, while adjusting the phase for a maximum signal. The photoelectric effect could be eliminated by double modulation, but in our apparatus it usually occurred almost 90° out of phase with the detachment signal, and hence caused no difficulty.

D. Electron Collection Efficiency

The electric and magnetic fields in the detachment chamber were studied both experimentally and analytically to ensure that all slow free electrons in the beam are collected. Figure 5 shows the saturation of photodetached electron current as a function of both the electric and magnetic field. The collection efficiency for electrons is unaffected by applying a 1.5-volt positive potential to the ion collector.

E. Procedure in Obtaining Data

Once the geometry of the optical system is fixed, the wave forms of the chopped light from the projection lamp and the mercury lamp are measured. The ion beam is then turned on and the 90° sector spectrometer verifies the mass spectral purity of the beam. The ion energy is measured. After calibrating the amplifier gain and determining the proper phase adjustments for the synchronous reference signal, a filter is put in place, the

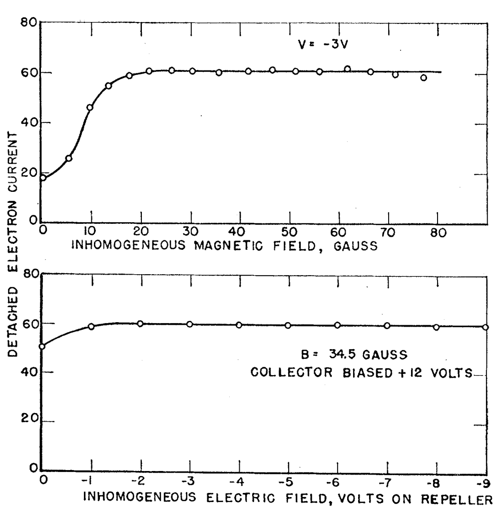

FIG. 5. The current to the electron collector saturates as the magnetic and electric fields in the reaction chamber are separately increased from zero demonstrating that all photodetached electrons are collected.

TABLE III. P_{exp}/P_{theor} averaged over a number of measurements for each of the nine filters, relative to the result obtained for filter 3486.

Corning filter No.	Approximate cutoff (A)	Relative P_{exp}/P_{theor}
3389	4200	0.96
3385	4800	1.02
3486	5300	...
3482	5500	0.97
2424	5900	0.98
2412	6100	1.02
2030	6600	1.00
2550	~8500	0.99
2540	~9900	0.97

projection lamp is turned on, and a set of about 6 photodetachment peaks is recorded. The amplifier gain is again calibrated, the sharp cutoff filter changed and the procedure repeated. At the close of the run the mass spectrum is rechecked and the energy redetermined.

VI. RESULTS

Photodetachment from H^- and D^- has been studied with sufficient variation in the parameters to show that Eq. (5) describes correctly the functioning of the apparatus. Data have been taken with variations of a factor of 4 in light power, a factor of 10 in ion current, and a factor of 2 in ion energy. The wave-form corrections have been deliberately exaggerated by masking parts of the optical system until the correction has increased from 3 percent to 15 percent. A wide variety of lamp and mirror geometries were used in an effort to cause lack of homogeneity in the light image to show up as a lack of reproducibility in the data rather than as a systematic error. The intensity distribution $\phi'(\lambda)$ was artificially altered in the visible region of the spectrum by the insertion of the nine sharp cutoff filters.

Under these conditions the reproducibility of the result, P_{exp}/P_{theor}, has a mean deviation of about 2 percent. There are many factors contributing to this scatter: (a) noise in the output signal; (b) gain instability; (c) phase adjustment; (d) spatial variations in ion and light beams; (e) different time constants associated with measurements of $\bar{j}$, i, and $\bar{W}$; (f) spectral distribution (for example, the temperature dependence of the filter transmissions); and (g) ion energy spread and instability.

The systematic errors are difficult to evaluate within definite upper limits. The following systematic errors are considered plausible (some of them having been discussed in Part III): (a) light power $\bar{W}\pm5$ percent; (b) $\int\sigma\phi'\lambda d\lambda\pm2$ percent; (c) ion velocity $v\pm1$ percent; (d) electron current, $\bar{j}$, including wave form, ±1.5 percent; (e) ion current $i\pm1$ percent; (f) radiometer height s, ±0.010 in. out of 0.400 in.$=\pm2.5$ percent. The uncertainty in s results from edge reflection effects. Should all these errors be present and influence the result in the same direction, an error of 13 percent would be present. As this is rather unlikely, we feel that our determination is reliable to within about 10 percent.

A number of absolute measurements were made under widely differing circumstances regarding the magnitudes of the relevant parameters. These data were taken with filters 3486 and 2412. The average of these values states that

$$P_{\text{exp}}/P_{\text{theor}} = 1.01 \ (\pm 0.02) \ (\pm 0.10).$$

Here the two figures in parenthesis are taken to describe the reproducibility of the result and to give an estimate of its reliability, respectively.

When the nine filters, with cutoff wavelengths ranging from 4250 to about 9000 A, were placed successively in the beam, the relative ratios of $P_{\text{exp}}/P_{\text{theor}}$ varied as shown in Table III. Filter 3389 has an absorption near the intensity peak, which causes the transmitted energy to be more sensitive to temperature than in the other filters. There is nothing in these data to suggest that the theoretical cross section is in error between 4000 and 9000 A.

VII. CONCLUSIONS

The theoretical value of the cross section for photodetachment of electrons from H^- has been confirmed experimentally, although this cross section could be modified by perhaps 10 percent without being adjudged in conflict with experiment. The method can be applied to other negative ions for the determination of electron affinities and photodetachment cross sections for those ions whose affinities lie in the range from 0.6 to 2.5 ev.

VIII. ACKNOWLEDGMENTS

The suggestions and interest of Professor O. Oldenberg, Professor E. M. Purcell, and Dr. W. L. Fite are gratefully acknowledged. The authors are also indebted to many members of the National Bureau of Standards staff who helped in the construction and calibration of the apparatus, particularly Adolph Huriaux, William McKean, and Victor Grob.

PHYSICAL REVIEW VOLUME 98, NUMBER 4 MAY 15, 1955

Zeeman Effect in the Rotational Spectrum of NO*

MASATAKA MIZUSHIMA, J. T. COX, AND WALTER GORDY
Department of Physics, Duke University, Durham, North Carolina
(Received November 8, 1954; revised manuscript received January 28, 1955)

The Zeeman splitting of the 2-mm wave, $J=1/2 \rightarrow 3/2$ rotational transit on of $N^{14}O^{16}$ in the $^2\Pi_{1/2}$ electronic state has been measured with fields of the order of 100 gauss. The observations were made with a wave-guide cell coiled between the poles of a Varian magnet. Magnetic field measurements were made with the electronic resonance of DPPH at frequencies of the order of 300 Mc/sec. A general theory of the Zeeman effect with hfs has been developed and applied specifically to $N^{14}O^{16}$. The g factors for the four states under investigation were found theoretically to be expressed as: $J=1/2$, $g_c=0.0007-\alpha$, $g_d=0.0007+\alpha$; $J=3/2$, $g_c=\bar{g}-\frac{2}{5}\alpha$, $g_d=\bar{g}+\frac{2}{5}\alpha$, where c and d are the lower and upper components of the Λ-type doublet, respectively. This relation was found to hold experimentally well with the values, $\bar{g}=-0.0230$ and $\alpha=+0.0025$. Theoretically, $\bar{g}$ comes from the mixing of $^2\Pi_{1/2}$ and $^2\Pi_{3/2}$ states and α comes from that of $^2\Pi_{1/2}$ and $^2\Sigma$ states. It was found by the theory, in which the centrifugal force and the spin orbit coupling were taken into account, that the electronic wave function of the two rotational states should be: $J=1/2$, $(^2\Pi_{1/2}|-0.0021(^2\Sigma|$; $J=3/2$, $(^2\Pi_{1/2}|-0.0247(^2\Pi_{3/2}|-0.0021(^2\Sigma|$. These wave functions give $\bar{g}$(theor.)$=-0.0229$ and and α(theor.)$=+0.0020$, which agree very well with the observed values. The observed g factor in $J=3/2$ state, $\bar{g}=0.0230$ Bohr magnetons, shows that in the supposedly "nonmagnetic" $^2\Pi_{1/2}$ state the NO molecule has a sizeable magnetic moment.

INTRODUCTION

NITRIC oxide is special among all stable molecules, since it has an odd number of electrons whereas all the others have an even number of electrons. This odd electron has an orbital rotational angular momentum $\hbar$ around the molecular axis in the ground state. The spin angular momentum of this electron is also strongly coupled to the molecular axis, resulting in $\Pi_{1/2}$ and $\Pi_{3/2}$ states, where $\Omega=1/2$ and $3/2$, respectively.[1] In the ground state $\Pi_{1/2}$ the magnetic moments due to the orbital motion and spin cancel, while in the $\Pi_{3/2}$ state, which is 121 cm^{-1} above the ground state, they give the resulting magnetic moment of 2 Bohr magnetons. The susceptibility data were explained well by these assumptions. The hfs data in the microwave spectra of this molecule observed by Gordy and Burrus[2] and Gallagher *et al.*[3] showed, how-

* This research was supported by the U. S. Air Force through the Office of Scientific Research of the Air Research and Development Command.

[1] For a review see, J. H. Van Vleck, *The Theory of Electric and Magnetic Susceptibility* (Oxford University Press, London, 1932), p. 269.
[2] C. A. Burrus and W. Gordy, Phys. Rev. **93**, 419 (1954).
[3] Gallagher, Bedard, and Johnson, Phys. Rev. **93**, 729 (1954).